

## Journal Pre-proof

Kinetic and thermodynamic study of c-Met interaction with single chain fragment variable (scFv) antibodies using phage based surface plasmon resonance



Farzaneh Ghorbani , Farzaneh Fathi , Leili Aghebati-Maleki ,  
Rozita Abolhasan , Reza Rikhtegar ,  
Jafar Ezzati Nazhad Dolatabadi , Zohreh Babaloo ,  
Balal Khalilzadeh , Majid Ebrahimi-Warkiani , Zahra Sharifzadeh ,  
Mohammad-Reza Rashidi , Mehdi Yousefi

PII: S0928-0987(20)30151-2  
DOI: <https://doi.org/10.1016/j.ejps.2020.105362>  
Reference: PHASCI 105362

To appear in: *European Journal of Pharmaceutical Sciences*

Received date: 7 December 2019  
Revised date: 19 March 2020  
Accepted date: 23 April 2020

Please cite this article as: Farzaneh Ghorbani , Farzaneh Fathi , Leili Aghebati-Maleki , Rozita Abolhasan , Reza Rikhtegar , Jafar Ezzati Nazhad Dolatabadi , Zohreh Babaloo , Balal Khalilzadeh , Majid Ebrahimi-Warkiani , Zahra Sharifzadeh , Mohammad-Reza Rashidi , Mehdi Yousefi , Kinetic and thermodynamic study of c-Met interaction with single chain fragment variable (scFv) antibodies using phage based surface plasmon resonance, *European Journal of Pharmaceutical Sciences* (2020), doi: <https://doi.org/10.1016/j.ejps.2020.105362>

This is a PDF file of an article that has undergone enhancements after acceptance, such as the addition of a cover page and metadata, and formatting for readability, but it is not yet the definitive version of record. This version will undergo additional copyediting, typesetting and review before it is published in its final form, but we are providing this version to give early visibility of the article. Please note that, during the production process, errors may be discovered which could affect the content, and all legal disclaimers that apply to the journal pertain.

© 2020 Published by Elsevier B.V.

**Kinetic and thermodynamic study of c-Met interaction with single chain fragment variable (scFv) antibodies using phage based surface plasmon resonance**

Farzaneh Ghorbani<sup>1, 2</sup>, Farzaneh Fathi<sup>3</sup>, Leili Aghebati-Maleki<sup>4</sup>, Rozita Abolhasan<sup>1</sup>, Reza Rikhtegar<sup>5</sup>, Jafar Ezzati Nazhad Dolatabadi<sup>6</sup>, Zohreh Babaloo<sup>7</sup>, Balal Khalilzadeh<sup>1</sup>, Majid Ebrahimi-Warkiani<sup>8</sup>, Zahra Sharifzadeh<sup>9</sup>, Mohammad-Reza Rashidi<sup>1</sup>, Mehdi Yousefi<sup>1, 5, 7</sup> \*

- 1 Stem Cell and Regenerative Medicine Institute (SCARM), Tabriz University of Medical Sciences, Tabriz, Iran
- 2 Student research committee, Tabriz University of Medical Sciences, Tabriz, Iran
- 3 Pharmaceutical Sciences Research Center, Ardabil University of Medical Sciences, Ardabil, Iran
- 4 Immunology Research Center, Tabriz University of Medical Sciences, Tabriz, Iran
- 5 Aging Research Institute, Tabriz University of Medical Sciences, Tabriz, Iran
- 6 Drug Applied Research Center, Tabriz University of Medical Sciences, Tabriz, Iran
- 7 Department of Immunology, Faculty of Medicine, Tabriz University of Medical Sciences, Tabriz, Iran
- 8 School of Biomedical Engineering, University Technology of Sydney, Sydney, New South Wales, 2007, Australia
- 9 Department of Immunology, Hybridoma Lab, Pasteur Institute of Iran, Tehran, Iran

**\*Corresponding author:**

Mehdi Yousefi, Ph.D of Immunology, Assistant Professor,  
Department of Immunology, Tabriz University of Medical Sciences, Tabriz, Iran  
PO Box: 6446-14155, Email: Yousefime@tbzmed.ac.ir

**Abstract**

Mesenchymal epithelial transition factor (c-Met) has been recently regarded as an attractive target for the treatment of cancer. Our previous study showed that c-Met-specific single chain fragment variables (scFvs) can be considered as a promising therapy for cancer, however, their molecular interaction with c-Met protein have not been assessed. Accordingly, in the current study we aim to evaluate the kinetic and thermodynamic properties of c-Met interaction with these scFvs as anticancer agents by means of surface plasmon resonance (SPR) technique. Phage-scFvs were immobilized on the 11-mercaptoundecanoic acid gold chips after carboxylic groups activation by N-ethyl-N-(3-diethylaminopropyl) carbodiimide/N-hydroxysuccinimide and, then the c-Met binding to each scFvs (ES1, ES2, and ES3) at different concentrations (ranging from 20 to 665  $\mu\text{M}$ ) was explored. Kinetic studies revealed that ES1 has the highest affinity ( $K_D = 3.36 \times 10^{-8}$ ) toward its target at 25 °C. Calculation of thermodynamic parameters also showed positive values for enthalpy and entropy changes, which was representative of hydrophobic forces between c-Met and ES1. Furthermore, the positive value of Gibbs free energy indicated that c-Met binding to ES1 was enthalpy-driven. Taken together, we concluded that produced ES1 can be applied as promising scFv-based therapy for diagnosis or targeting of c-Met in various cancers.

**Keywords:** c-Met; scFv; cancer

## 1. Introduction

Mesenchymal epithelial transition factor (c-Met) is a unique tyrosine kinase receptor for hepatocyte growth factor (HGF) which is consisted of extracellular  $\alpha$  and transmembrane  $\beta$  chains and is involved in a wide array of cellular processes including scattering, proliferation, migration, differentiation, motility, and angiogenesis [1, 2]. Anomalous c-Met activation or signaling has been noted in a variety of tumor types [3]. Therefore, molecular targeting of c-Met receptor is a promising therapeutic approach for cancer treatment that is becoming more and more popular with recent various therapeutic strategies undergoing clinical trials [4, 5]. For example, monoclonal antibodies (MAbs) against c-Met have been effectively employed in the clinical therapy of various cancer cells because of their high specificity and low toxicity [6].

Single-chain variable fragment (scFv) is a 28-30 KDa fusion protein, which is combined of variable regions of the heavy (VH) and light (VL) chains of an antibody connected with a peptide linker. Due to their smaller size and rapid tissue penetration, scFvs are expected to be more efficient than MAbs in treatment and imaging of tumor tissues [7, 8]. Moreover, the generation of scFv antibodies appears to be more cost-effective than that of whole immunoglobulins [9]. It has also been reported that anti-c-Met-scFv-mediated delivery of drug could be a great potential strategy in targeted therapy and imaging of tumor cells [10]. In our previous study also three scFvs (ES1, ES2, and ES3) were isolated from Tomlinson I+J library against a specific oligopeptide from Sema domain of the c-Met via phage display technique [7]. These scFvs showed great therapeutic promise in colorectal cancer immunotherapy. ES1 and ES2 could effectively inhibit the human colorectal carcinoma cell line (HCT-116) proliferation. The results also demonstrated that ES1, ES3 and ES2 had the most apoptotic effect on HCT-116,

respectively. However, an understanding of the precise molecular mechanism of the action of these scFvs on c-Met may contribute to successful drug development in the future clinical trials.

Surface plasmon resonance (SPR) is a powerful label-free technique used to investigate biomolecular interactions such as drug-protein, antibody-antigen, protein-DNA and also cellular morphological changes in real time [11-13]. Determination of thermodynamic parameters and kinetic constants including association and dissociation rate and affinity is also possible using this tool [14]. Since SPR signal intensity is proportional to the mass at the sensor surface [15], phage-displayed scFvs could be more suitable for interaction analysis instead of the scFv fragments alone. Furthermore, they have multiple advantages over antibodies including easy production, high stability and insensitivity to temperature, pH, and ionic strength [16].

Considering these observations, we intended to evaluate the kinetic constants of interaction between c-Met with the three mentioned scFvs (ES1, ES2 and ES3) from our previous study for future application in cancer treatment using phage-based SPR technique. Furthermore, we calculated thermodynamic parameters for the scFv which had the highest affinity for the c-Met protein.

## **2. Materials and methods**

### ***2.1. Reagents and materials***

A synthetic immunodominant peptide from the Sema domain of c-Met (AQLARQIGASLND) was prepared from JPT (JPT Peptide Technologies GmbH Berlin, Germany). Three M13 phage clones with different anti-c-Met scFvs including ES1, ES2, and ES3 displayed on their protein pIII, were purified from a phage display Tomlinson I + J library in our previous study [7]. *E. coli*

TG1 (Novagen, Madison, WI) was employed as host for phagemid manipulation. M13KO7 helper phage was obtained from BioScience, Nottingham (UK). 11-mercaptoundecanoic acid (11-MUA), ethanolamine, N-hydroxy succinimide (NHS) and 1-ethyl-3-[3-dimethylaminopropyl] carbodiimide Hydrochloride (EDC), bovine serum albumin (BSA), phosphate buffered saline (PBS), and ammonia were prepared from Sigma–Aldrich Steinheim, Germany. Gold chips were supplied from BioNavis Company (Tampere, Finland).

## ***2.2. Phage amplification***

Briefly, 100  $\mu$ L of each phage clone was added in 50 ml 2xYT (16 g Tryptone, 5 g NaCl and 10 g Yeast Extract in 1 liter) containing 120 mg/ml ampicillin and incubated with shaking (250 rpm) at 37 °C until OD600 reach to 0.4–0.5. M13K07 helper phages ( $5 \times 10^{11}$  plaque forming units (PFUs)) were then added to per milliliter of bacterial culture and incubated for 30 minutes at 37 °C without shaking and for another additional 30 minutes under shaking (at 100 rpm). Next, infected bacteria were collected by centrifuging (3800 rpm at 4 °C for 10 min), re-suspended in 100 ml of fresh 2xYT supplemented with 50  $\mu$ g/ml kanamycin and 120  $\mu$ g/ml ampicillin and incubated overnight at 30 °C under shaking (at 200 rpm). Finally, phages were precipitated from the supernatant with PEG-6000/2.5 M NaCl and collected by centrifugation (at 14000 rpm at 4 °C for 20 min).

## ***2.3. SPR instrument and technique***

The kinetic and thermodynamic parameters were recorded using a SPR device with dual-channel detection which utilizes the Kretschman prism configuration (MP-SPR Navi 210A, BioNavis

Ltd, Tampere-region, Finland). Prior to the SPR experiment, the whole flow path was rinsed with PBS–0.02% Tween (PH=7.2) as running buffer. The interaction analysis was performed in the fixed angle at 670 nm wavelength and 25°C temperature.

#### ***2.4. Preparation of gold chips***

The material of the SPR-Navi gold sensor chips is 240 mm<sup>2</sup> BK7 glass, with 50 nm gold layers evaporated onto their surface. To eliminate any contamination and obtain more accurate data, the bare gold slides were dipped in a 1:1:5 mixture of ammonia (NH<sub>4</sub>OH, 25%), hydrogen peroxide (H<sub>2</sub>O<sub>2</sub>, 30%), and deionized water for about 15 minutes at 100°C. Following the immersion of the chips in ethanol for 5 minutes at 95°C, they were thoroughly washed with deionized water and dried by N<sub>2</sub> atmosphere.

It has been found that the quantity of immobilized M13 phages is much higher on the 11-MUA coated chips than that on CM5 chips [17]. Therefore, in order to form a self-assembly carboxyl terminated monolayer on the cleaned gold slides surface, we used the protocol described by Liu et al. (2009). Briefly, we submerged the gold chips in the of 50 mM 11-MUA solution prepared in 70% ethanol at 25°C for 24 hours and then the 11-MUA coated chips were washed with ethanol and PBS buffer and then dried by N<sub>2</sub>. Finally, prepared chips were placed on the SPR instrument for the following phage immobilization.

#### ***2.5. Phage immobilization via amino coupling***

Phages were covalently immobilized onto the gold coated 11-MUA chips through standard amine coupling chemistry. Briefly, the carboxyl groups on the 11-MUA chip was activated by a 1:1 mixture of 200 mM EDC and 50 mM NHS solution at a flow rate of 15  $\mu\text{L}/\text{min}$  for 8 minutes. Phage solutions at four different concentrations ( $1.5 \times 10^8$ ,  $2 \times 10^8$ ,  $2.5 \times 10^8$ , and  $3 \times 10^8$  pfu/mL) were prepared with PBS–0.02% Tween (pH 7.2) to find the optimized concentration and injected into the sensing channel over the activated chip surface for 15 minutes at a flow rate of 8  $\mu\text{L}/\text{min}$ . Finally, 1 M ethanolamine solution was injected over the chip surface for blocking residual activated groups using a flow rate of 20  $\mu\text{L}/\text{min}$  for 3 minutes.

#### ***2.6. Assessment the specificity of the chip***

To investigate the specificity of the c-Met interaction with the immobilized phage-scFvs, three samples including PBS (as running buffer), 33  $\mu\text{M}$  BSA protein (as negative control), and 33  $\mu\text{M}$  c-Met (as positive control), were injected over the phage surface using a flow rate of 10  $\mu\text{L}/\text{min}$  for 5 min.

#### ***2.7. Kinetic analysis of c-Met interaction with ES1, ES2 and ES3***

To determine the kinetic parameters for each interaction, different concentrations of the c-Met (20 to 665  $\mu\text{M}$ ) prepared with PBS–0.02% Tween buffer at pH 7.2 were injected into the both sensing and reference channels at the same time using a flow rate of 10  $\mu\text{L}/\text{min}$  for 5 min. Due to the quick dissociation of the peptide from scFvs, regeneration process was not required. Eventually, data was extracted with SPR Navi<sup>TM</sup> data viewer software and Trace Drawer<sup>TM</sup> for

SPR Navi<sup>TM</sup> was employed for calculation of kinetic and affinity parameters of c-Met binding to the scFvs.

### ***2.8. Thermodynamic analysis of c-Met binding to the scFv with the highest affinity***

The effect of temperature on c-Met binding to the scFv with the best affinity was investigated by calculation of c-Met–scFv complex formation thermodynamic parameters. To this aim, SPR evaluations were studied at three different temperatures (298, 303, and 310 K).

## **3. Results**

### ***3.1. Phage immobilization through amine coupling***

In order to detect the interaction between the c-Met peptide and three different c-Met-specific scFvs (ES1, ES2, and ES3) expressed on M13 phages, we used SPR technique. We immobilized the phages by amine coupling method as illustrated in Figure 1. For this aim, a SAM of MUA, which has been previously found very suitable for M13 phage immobilization [17], was formed on the gold surface of chip and then EDC/NHS solution was used for activation of carboxylic groups (-COOH). Subsequently, the phages were easily stabilized on 11-MUA chip via covalent amide and electrostatic binding formation [18]. Sensorgram measurements of the aforementioned process approved that phage immobilization via amine coupling on 11-MUA chip was successfully done (Figure 2a). The SPR responses unit (RU) caused by phage binding was 0.058RU which shows proper and acceptable phage immobilization level. In addition to the time and flow rate of injection, the concentration of phages can also considerably affect the efficiency

of immobilization process. In this regard, we found  $3 \times 10^8$  pfu/mL as the optimum concentration of phages (Figure 2b). Finally, the unreacted sites of the surface were blocked with ethanolamine.

### **3.2. Specificity of the chip**

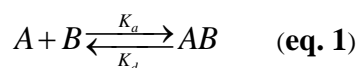
As shown in Figure 2c and Figure S1, there was no specific interaction between PBS and the immobilized scFvs. Also, as shown in Figure S1 after stopping the injection of BSA on immobilized scFvs surface, the related sensogram reached near the baseline surface like PBS, however, after stopping the c-Met injection, it absorbed on surface and did not reach to the initial level ( $0.0012 \text{ RU} \pm 0.0005$ ). These results showed the considerable specificity of scFvs toward c-Met peptide.

### **3.3. Interaction of c-Met with ES1, ES2, and ES3**

The sensograms of interaction between each ES1, ES2, and ES3 with different concentrations of c-Met (between 20 to 665  $\mu\text{M}$ ) at 25 °C are presented in Figure 3a, b, and c, respectively. Also the fitted models of related sensograms were shown in Figure S2.

### **3.4. Kinetics of c-Met binding to ES1, ES2, and ES3**

Kinetic parameters elucidate the interaction rate of c-Met binding to ES1, ES2, and ES3. The formation and decomposition of the complex (AB) between c-Met (A) and scFvs (B) is calculated by equation 1.



Association and dissociation rate constants ( $k_a$  and  $k_d$ ) are two kinetic parameters represent the number of AB formed and decayed per second, respectively that were analyzed by means of SPR measurements [19]. The affinity or equilibrium constants ( $K_D$ ) which determines amount of AB complex formed at equilibrium for the bindings of c-Met to ES1, ES2, and ES3, were also evaluated from the eq. 2 [20].

$$K_D = \frac{k_d}{k_a} \quad (\text{eq. 2})$$

Table 1 summarized the kinetic parameters ( $k_a$ ,  $k_d$  and  $K_D$ ) of each interaction.

### 3.5. Thermodynamic study of c-Met interaction with ES1

The interaction type between c-Met and ES1 was detected by two thermodynamic parameters including enthalpy ( $\Delta H$ ) and entropy ( $\Delta S$ ) change values, which can be calculated using van't Hoff equation (eq. 3) by plotting of  $\ln K_D$  versus  $1/T$  [21].

$$\ln k_D = -\frac{\Delta H}{RT} + \frac{\Delta S}{R} \quad (\text{eq. 3})$$

R demonstrates the universal gas constant and T is indicative of absolute temperature.

As presented in sensograms of Figure 4 and fitted models in Figure S3, the c-Met binding to ES1 was studied at three different temperatures (298, 303, and 310 K). Figure 5 also represents the plot of  $\ln K_D$  versus  $1/T$ . By calculation of  $\Delta H$  and  $\Delta S$ , the total energy released from the interaction can be obtained through the standard Gibbs–Helmholtz equation (eq. 4).

$$\Delta G = \Delta H - T\Delta S \quad (\text{eq. 4})$$

Table 2 shows the thermodynamic parameters of c-Met-ES1 complex.

#### 4. Discussion

Since aberrant c-Met activation is associated with both tumor growth or formation, this protein has been regarded as an attractive target for cancer therapy and drug development [22].

Accurate determination of kinetic and thermodynamic parameters between the therapeutic agents and c-Met may result in better pharmacological response and clinical development. Currently, several methods especially isothermal titration calorimetry (ITC) and fluorescence polarization (FP) have been developed for evaluating molecular interactions [23]. ITC is a non-destructive technique, however, is not able to investigate the kinetics of non-enzyme perturbation and require large amount of sample and appropriate suite to evaluate data [23, 24]. There are also disadvantages of FP, as fluorescent-labelled ligand may change the binding affinity in this assay [23]. SPR has also been extensively used for detecting binding affinities due to their beneficial properties including low sample consumption, short assay development time, and ability in label-free and real-time sensing [25]. Measurement of higher binding affinities is also feasible by this technique [23]. Nevertheless, application of this tool demands high level of technical expertise.

Accordingly, in this study, we attempted to analyze the kinetic and thermodynamic parameters between c-Met and the scFv antibodies via phage based SPR. The reason why phage-scFvs were immobilized on the chips rather than scFvs alone was that the small change in the mass contributes to low refractive index changes and subsequently poor SPR signals. Moreover, phages have found to be more stable to the thermal and pH changes than antibodies or scFvs and can be easily produced [16].

Several studies have assessed the binding affinities between human c-Met protein and various antibodies introduced as a main class of drugs. The low value of  $K_D$  is representative of high tendency between two molecules. For instance, in 2012, Oh et al. found that F46, a mouse MAb, could bind to c-Met with high affinity ( $K_d = 2.56 \times 10^{-9}$ ), as determined by SPR and successfully decrease *in vivo* tumor growth [26]. Merchant et al. developed a potent monovalent anti-c-Met agonistic antibody (onartuzumab), which showed high affinity ( $K_D = 1.2 \times 10^{-9}$ ) towards wild type human c-Met as evaluated by SPR [27]. Furthermore, SHR-A1403, a novel c-Met antibody-drug conjugate, could bind to human c-Met with high affinity ( $K_D = 1.71 \times 10^{-8}$ ) and is considerable as potential agent for treatment of cancers with high c-Met levels [28]. In another study conducted by Park et al. (2017), IRCR201, a novel fully-human bivalent antibody, exhibited high affinity to human c-Met ( $K_D = 7.207 \times 10^{-8}$ ) and provided an ideal anti-tumor activity for treatment of c-Met-positive cancer patients [29]. A Phase I clinical trial was also designed by Park et al. to investigate the pharmacokinetic profile, safety and efficiency of SAIT301, a novel humanized Mab, for treatment of patients with c-Met-positive solid tumors. SAIT301 was intravenously administrated to the patients in 21 day cycles, for up to 4 cycles. This study is still ongoing and is not so far ended (ClinicalTrials.gov identifier: NCT02296879; Park et al., 2015).

Nevertheless, scFvs, as small antibody fragments, could penetrate more deeply and rapidly to the tumor tissues and effectively reach to their targets than whole antibodies [30]. Besides, due to their fast blood clearance rate, scFvs can be utilized appropriately to deliver drugs, toxins or radionuclides to the target tissues [31]. Lu and coworkers have been demonstrated the high binding affinity between the c-Met protein and three anti-cMet scFv antibodies including Ms1 ( $K_D = 6.82 \times 10^{-9}$ ), Ms20 ( $K_D = 9.14 \times 10^{-9}$ ), and Ms21 ( $K_D = 14.9 \times 10^{-9}$ ) as measured by SPR.

The drug delivery system mediated by these scFvs showed a great promise in targeted therapy and imaging of tumor tissues associated with overexpression of c-Met [10]. Our results also revealed that ES1 ( $K_D = 3.36 \times 10^{-8}$ ), ES2 ( $K_D = 1.02 \times 10^{-7}$ ) and ES3 ( $K_D = 7.84 \times 10^{-6}$ ) have the highest affinity towards c-Met at 25 °C, respectively (Table 1). These data suggest that ES1 may act as more potent anti-tumor agent in treatment of c-Met-positive cancers.

We further detected the interaction type between c-Met and ES1 which showed the most anti-proliferative and apoptotic properties on HCT-116 cells [7] and had the most affinity toward c-Met in comparison with ES2 and ES3. Hydrophobic forces, hydrogen bond, Van der Waals and electrostatic interactions are types of binding force between the biomolecules. The positive value of both  $\Delta H$  and  $\Delta S$  indicates the occurrence of hydrophobic forces; negative values mark the Van der Waals interactions and hydrogen bonds. The electrostatic interaction is also characterized by the negative  $\Delta H$  along with positive amount of  $\Delta S$  [32]. According to the obtained data from this study, positive values of  $\Delta H$  and  $\Delta S$  which was indicated that the interaction between c-Met and ES1 occurs through hydrophobic binding forces. Besides, the positive value of  $\Delta G$  indicated that the binding process was enthalpy driven and the formation of c-Met-ES1 complex was the kind of endothermic process. The results of this study also showed that a small temperature rise led to the decrease in the binding affinity between ES1 and c-Met (Table 2).

## 5. Conclusion

In this study, we investigated the kinetic parameters of c-Met interaction with three c-Met-specific scFvs (ES1, ES2, and ES3) using the SPR technique. Kinetic parameters showed that ES1 and then ES2 and ES3 have the highest affinity for the c-Met peptide, respectively which

was approved by the  $K_D$  values. We further studied the thermodynamic parameters between c-Met and ES1 which was indicated that the dominant force in this interaction refers to hydrophobic forces. In addition, the binding process was endothermic due to the positive value of  $\Delta G$ . Taken together, we concluded that ES1 could more be considered as a promising anti-tumor agent among the other scFvs. However, future *in vitro* and *in vivo* studies are still needed to further investigate its properties.

#### Declarations of interest

None.

#### Acknowledgment

This work has been done as part of the M.Sc. thesis for Farzaneh Ghorbani and was supported by Stem Cell Research Center, Tabriz University of Medical Sciences, Iran [Grant NO. 60931].

#### References

1. Safaie Qamsari, E., et al., *The c-Met receptor: Implication for targeted therapies in colorectal cancer*. *Tumour Biol*, 2017. 39(5): p. 1010428317699118.
2. Ricci, G. and A. Catizone, *Pleiotropic Activities of HGF/c-Met System in Testicular Physiology: Paracrine and Endocrine Implications*. 2014. 5(38).
3. Organ, S.L. and M.-S. Tsao, *An overview of the c-MET signaling pathway*. *Therapeutic advances in medical oncology*, 2011. 3(1 Suppl): p. S7-S19.
4. Shali, H., et al., *IGF1R and c-met as therapeutic targets for colorectal cancer*. *Biomed Pharmacother*, 2016. 82: p. 528-36.
5. Porter, J., *Small molecule c-Met kinase inhibitors: a review of recent patents*. *Expert Opin Ther Pat*, 2010. 20(2): p. 159-77.

6. Greenall, S.A., et al., *Non-agonistic bivalent antibodies that promote c-MET degradation and inhibit tumor growth and others specific for tumor related c-MET*. *PLoS One*, 2012. 7(4): p. e34658.
7. Qamsari, E.S., et al., *Isolation and characterization of anti c-met single chain fragment variable (scFv) antibodies*. *J Immunotoxicol*, 2017. 14(1): p. 23-30.
8. Edwardraja, S., et al., *Redesigning of anti-c-Met single chain Fv antibody for the cytoplasmic folding and its structural analysis*. *Biotechnol Bioeng*, 2010. 106(3): p. 367-75.
9. Heo, M.A., et al., *Functional expression of single-chain variable fragment antibody against c-Met in the cytoplasm of Escherichia coli*. *Protein Expr Purif*, 2006. 47(1): p. 203-9.
10. Lu, R.M., et al., *Single chain anti-c-Met antibody conjugated nanoparticles for in vivo tumor-targeted imaging and drug delivery*. *Biomaterials*, 2011. 32(12): p. 3265-74.
11. Atale, S.S., et al., *Understanding the nano-bio interactions using real-time surface plasmon resonance tool*. *International Journal of Biological Macromolecules*, 2019. 123: p. 97-107.
12. Mulla, T., S. Patil, and J. Jadhav, *Exploration of surface plasmon resonance for yam tyrosinase characterization*. *Int J Biol Macromol*, 2018. 109: p. 399-406.
13. Fathi, F., et al., *Detection of CD133-marked cancer stem cells by surface plasmon resonance: Its application in leukemia patients*. *Biochim Biophys Acta Gen Subj*, 2019. 1863(10): p. 1575-1582.
14. Fathi, F., et al., *Kinetic and thermodynamic insights into interaction of albumin with piperacillin: Spectroscopic and molecular modeling approaches*. *Journal of Molecular Liquids*, 2019. 296: p. 111770.
15. Fathi, F., M.-R. Rashidi, and Y. Omid, *Ultra-sensitive detection by metal nanoparticles-mediated enhanced SPR biosensors*. *Talanta*, 2019. 192: p. 118-127.
16. Naidoo, R., et al., *Surface-immobilization of chromatographically purified bacteriophages for the optimized capture of bacteria*. *Bacteriophage*, 2012. 2(1): p. 15-24.
17. Liu, F., et al., *Phage-displayed protein chip based on SPR sensing*. *Sensors and Actuators B: Chemical*, 2009. 136(1): p. 133-137.
18. Jordan, C.E. and R.M. Corn, *Surface Plasmon Resonance Imaging Measurements of Electrostatic Biopolymer Adsorption onto Chemically Modified Gold Surfaces*. *Anal Chem*, 1997. 69(7): p. 1449-56.
19. Jonsson, U., et al., *Real-time biospecific interaction analysis using surface plasmon resonance and a sensor chip technology*. *Biotechniques*, 1991. 11(5): p. 620-7.
20. Rispens, T., et al., *Label-free assessment of high-affinity antibody-antigen binding constants. Comparison of bioassay, SPR, and PEIA-ellipsometry*. *Journal of immunological methods*, 2011. 365: p. 50-7.
21. Yasseen, Z.J., J.H. Hammad, and H.A. Altalla, *Thermodynamic analysis of thymoquinone binding to human serum albumin*. *Spectrochimica acta. Part A, Molecular and biomolecular spectroscopy*, 2014. 124: p. 677-681.
22. Mo, H.-N. and P. Liu, *Targeting MET in cancer therapy*. *Chronic diseases and translational medicine*, 2017. 3(3): p. 148-153.
23. Du, X., et al., *Insights into Protein-Ligand Interactions: Mechanisms, Models, and Methods*. *International journal of molecular sciences*, 2016. 17(2): p. 144.
24. Su, H. and Y. Xu, *Application of ITC-Based Characterization of Thermodynamic and Kinetic Association of Ligands With Proteins in Drug Design*. *Frontiers in pharmacology*, 2018. 9: p. 1133-1133.
25. Nagata, K. and H. Handa, *Real-Time Analysis of Biomolecular Interactions: Applications of BIACORE*. 2000.
26. Oh, Y.M., et al., *A new anti-c-Met antibody selected by a mechanism-based dual-screening method: therapeutic potential in cancer*. *Molecules and cells*, 2012. 34(6): p. 523-529.

27. Merchant, M., et al., *Monovalent antibody design and mechanism of action of onartuzumab, a MET antagonist with anti-tumor activity as a therapeutic agent*. *Proc Natl Acad Sci U S A*, 2013. 110(32): p. E2987-96.
28. Yang, C.Y., et al., *SHR-A1403, a novel c-Met antibody-drug conjugate, exerts encouraging anti-tumor activity in c-Met-overexpressing models*. *Acta Pharmacol Sin*, 2019. 40(7): p. 971-979.
29. Park, H., et al., *Tumor Inhibitory Effect of IRCR201, a Novel Cross-Reactive c-Met Antibody Targeting the PSI Domain*. *International journal of molecular sciences*, 2017. 18(9): p. 1968.
30. Ahmad, Z.A., et al., *scFv antibody: principles and clinical application*. *Clin Dev Immunol*, 2012. 2012: p. 980250.
31. Colcher, D., et al., *Pharmacokinetics and biodistribution of genetically-engineered antibodies*. *Q J Nucl Med*, 1998. 42(4): p. 225-41.
32. Xu, J., H.Q. Yu, and G.P. Sheng, *Kinetics and thermodynamics of interaction between sulfonamide antibiotics and humic acids: Surface plasmon resonance and isothermal titration microcalorimetry analysis*. *J Hazard Mater*, 2016. 302: p. 262-266.

## Figure legends

**Figure 1.** Schematic illustration of phage immobilization by amine coupling; **1)** Formation of self-assembled monolayers (SAM) of MUA. **2)** Activation of –COOH in MUA by EDC/NHS. **3)** Immobilization of the phage. **4)** Blocking of the remaining activated surface groups by ethanolamines. **5)** Interaction of phage-scFvs with c-Met.

**Figure 2.** **a)** SPR sensogram of phage immobilization process on a MUA chip; **Cleaning:** cleaning of the chip surface with NaCl (2 M) and NaOH (0.1 M). **Activation:** activation of MUA chip surface through injection of NHS/EDC (1:1). **Immobilization:** Immobilization of  $3 \times 10^8$  pfu/mL phage. **Blocking:** blocking of the non-specific binding with ethanolamine. **b)** The response curves of phage immobilization at various concentrations. **c)** The response curves of the interaction between the phage-immobilized scFvs with different samples: PBS, BSA, and c-Met.

**Figure 3.** Sensogram of c-Met interaction with immobilized **a)** ES1, **b)** ES2, and **c)** ES3 at different concentrations (20 to 665  $\mu$ M) at 25 °C.

**Figure 4.** Sensogram of c-Met interaction with ES1 at different temperature **a)** 298 °K, **b)** 303 °K, **c)** 310 °K.

**Figure 5.** Van't Hoff plot for the interaction of c-Met with ES1.

Journal Pre-proof